Korean J. of Chem. Eng., **6**(3) (1989) *246-253*

NECKING IN ISOTHERMAL MELT SPINNING AND ITS CONNECTION TO THE VORTEX FORMATION IN ENTRANCE FLOW

Jae Chun HYUN

Department of Chemical Engineering, Korea University, Anam-Dong, Sungbuk-Ku, Seoul, Korea

(Received 11 February 1989 • accepted 27 March 1989)

Abstract—We derive the necking condition in isothermal melt spinning employing the model of convected Maxwell fluids with strain-rate dependent material relaxation time. It is found that necking is possible when the extensional viscosity is strain-thinning (strain-softening), and impossible when the extensional viscosity is strain-thickening (strain-hardening). This finding then immediately reveals the correspondence between the spinning process and entrance flow (contraction flow), as several recent articles show that vortex is formed in the entrance flow when the extensional viscosity is strain-thickening. Thus necking in spinning corresponds to no vortex in entrance flow, whereas no necking in spinning to vortex in entrance flow, for the flow mechanism of the both situations is the extensional flow whose behavior is determined by the extensional viscosity.

INTRODUCTION

Solid samples show necking phenomenon when the materials possess multi-valued stress-strain curves and the applied stress is greater than the material's critical necking stress as discussed by many people (e.g., Vincent[1] and Wada [2]). In the threadline of melt spinning, similar necking phenomena also have been observed and discussed by Ziabicki [3], Kase [4], Kikutani [6] and Maeda [5].

However, to date there has not been an in-depth theoretical study about this necking in the spinning threadline, as to how and why such phenomena occur, i.e., the necking conditions and rheological interpretation. In this study, we hence derive the necking condition for isothermal melt spinning using the simple governing equations of the system, which includes the model of convected Maxwell fluids with White's strain-rate dependent material relaxation time. Thus obtained results also reveal that depending on the value of the model parameter, "a" (strain-rate dependency of the material relaxation time), "necking" can occur in the threadline, manifested as the discontinuity of the threadline velocity (equivalently, the discontinuity of the threadline cross-sectional area).

Along with the necking condition, we derive the extensional viscosity as a function of extensional strain-rate, which provides a basic ground for the rheological understanding of the phenomenon. The behavior of this extensional viscosity is compared with that in entrance flow, as related to the formation of vortex in entrance flow. Namely, the fact that strain-thickening fluids generally exhibit vortex and strain-thinning fluids do not, can be interpreted as an evidence that the vortex phenomenon and the necking phenomenon are probably governed by the same kinematical mechanism. In other words, the fluids having larger "a" values and thus strain-thinning extensional viscosity, exhibit necking in spinning and no vortex in entrance flow, whereas the fluids having smaller "a" values and strain-thickening extensional viscosity, no necking in spinning and vortex in entrance flow.

The dichotomy of fluids by these two different types, is further discussed in terms of different behavior patterns in other flow situations.

DERIVATION OF THE NECKING CONDITION IN ISOTHERMAL MELT SPINNING

We begin with the same governing equations of isothermal spinning as those appeared in earlier articles (e.g., Hyun [7], Hyun & Ballman [8], and Hyun [9]). The same assumptions are also adopted here. 1) The secondary forces such as inertia, surface tension, air drag, and gravity are neglected. 2) The origin of the coordinate system starts at the die swell region. 3) The velocity distribution across the threadline cross-section is uniform. 4) We consider stress, velocity and so on in the axial direction only.

Then the one-dimensional model of isothermal melt spinning is as follows.

Continuity equation:

$$\left(\frac{\partial A}{\partial t}\right)_x+\left(\frac{\partial (Av)}{\partial x}\right)_t=0 \tag{1}$$

Equation of motion:

$$\frac{\partial}{\partial x}(A\sigma)_t=0 \tag{2}$$

Constitutive equation (convected Maxwell fluids):

$$\sigma+\lambda\left[v\left(\frac{\partial \sigma}{\partial x}\right)_t-2\sigma\left(\frac{\partial v}{\partial x}\right)_t\right]=2G\lambda\left(\frac{\partial v}{\partial x}\right)_t \tag{3}$$

Strain-rate dependent mateiral relaxation time (Ide & White [10]):

$$\lambda=\lambda_o/[1+a\sqrt{3}\lambda_o(\partial v/\partial x)_t] \tag{4}$$

where "a" is the material parameter representing the degree of the strain-rate dependency of the material relaxation time, λ.

The steady-state solution of the above equations (as shown in Hyun [9]) is, from Eqns. (1) and (2),

$Av=Q=$ constant = steady-state throughput

$A\sigma=F=$ constant = steady-state threadline tension force and from Eqns. (3) and (4),

$$\left(\frac{F}{Q}\right)v+\frac{\lambda_o}{1+a\sqrt{3}\lambda_o\left(\frac{\partial v}{\partial x}\right)_t}\left[v\left(\frac{F}{Q}\right)\left(\frac{\partial v}{\partial x}\right)_t-2\left(\frac{F}{Q}\right)v\left(\frac{\partial v}{\partial x}\right)_t\right]=\frac{2G\left(\frac{\partial v}{\partial x}\right)_t\lambda_o}{1+a\sqrt{3}\lambda_o\left(\frac{\partial v}{\partial x}\right)_t} \tag{5}$$

and $(\partial v/\partial x)_t = dv/dx$ at steady state.

Simplifying the above equation, we get

$$v+(dv/dx)[a\sqrt{3}\lambda_o v-\lambda_o v-2G\lambda_o(Q/F)]=0 \tag{6}$$

and

$$(dv/dx)=v/\{\lambda_o[K+v(1-a\sqrt{3})]\}, \tag{7}$$

where

$$K=(2GQ)/F=\text{a reciprocal tension force.} \tag{8}$$

Integrating Eqn. (7) from the spinneret ($x=0$, $v=v_o$) to the position of x, v, we obtain

$$x=\lambda_o K\ln(v/v_o)+\lambda_o(1-a\sqrt{3})(v-v_o) \tag{9}$$

And the expression for K can be obtained from Eqn. (9) by using the boundary condition at the take-up, i.e., at

$$x=L,\ v=v_L=rv_o \tag{10}$$

where

$$r=\text{draw-down ratio}=v_L/v_o=A_o/A_L. \tag{11}$$

$$K=\frac{L-\lambda_o(1-a\sqrt{3})v_o(r-1)}{\lambda_o\ln r}$$

$$=\frac{v_o[1-\bar{\lambda}_o(1-a\sqrt{3})(r-1)}{\bar{\lambda}_o\ln r}$$

$$=\frac{v_o[1+\beta(r-1)]}{\bar{\lambda}_o\ln r} \tag{12}$$

where

$$\bar{\lambda}_o\equiv(\lambda_o v_o)/L,\ \beta\equiv\bar{\lambda}_o(a\sqrt{3}-1). \tag{13}$$

We notice here that the reciprocal force K has the same dimension as velocity, v_o.

Upon substitution of Eqn. (12) into Eqn. (9), we get

$$x=\lambda_o v_o[1+\beta(r-1)]\ln(v/v_o)/(\bar{\lambda}_o\ln r)+\lambda_o(1-a\sqrt{3})v_o(v/v_o-1)$$

or

$$x/L=\{[1+\beta(r-1)]/\ln r\}\ln\xi-\beta(\xi-1) \tag{14}$$

where

$$\xi\equiv v/v_o \tag{15}$$

Eqn. (14) is the implicit expression of the threadline velocity, v (or ξ),in terms of the distance from the spinneret, x, i.e., Eulerian expression of v. The Lagrangian expression of v, i.e., in terms of the fluid element traveling time from the spinneret, τ, can be readily calculated as follows. From Eqn. (7), we get

$$dx/v=\{\lambda_o[K+v(1-a\sqrt{3})]/v^2\}dv \tag{16}$$

and so

$$\tau\equiv\int_0^x\frac{dx}{v}=\int_{v_o}^{v}\frac{\lambda_o[K+v(1-a\sqrt{3})]}{v^2}dv$$

$$=(\lambda_o K/v_o)(1-v_o/v)+\lambda_o(1-a\sqrt{3})\ln(v/v_o) \tag{17}$$

The substitution of Eqn. (12) into Eqn. (17) yields

$$\tau=(\lambda_o/v_o)(1-v_o/v)v_o[1+\beta(r-1)]/(\bar{\lambda}_o\ln r)+\lambda_o(1-a\sqrt{3})\ln(v/v_o)$$

The dimensionless Lagrangian time becomes as follows using Eqn. (13).

$$\tilde{\tau}\equiv\tau v_o/L=\{[1+\beta(r-1)]/\ln r\}(1-1/\xi)-\beta\ln\xi \tag{18}$$

Eqn. (18) shows the implicit expression of the threadline velocity, v (or ξ), in terms of the fluid traveling time from the spinneret, i.e., Lagrangian expression [See Hyun & Ballman [8] for the case of constant relaxation time, i.e., $a=0$ for Eqn. (4)].

Now we proceed to find the necking condition in the threadline from Eqn. (14) [Eqn. (18) could be used, but it is easy here to use the Eulerian expression to find the necking (discontinuity in velocity and cross-sectional area)]. As shown in Eqn. (14), β and r are the parameters which are involved in finding the necking phenomenon. Specifically, as shown by the case (3)

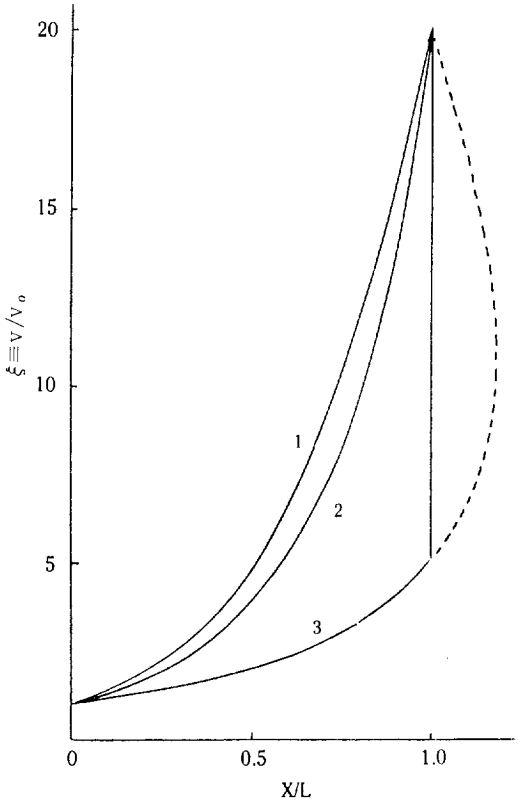

Fig. 1. Eulerian plots of dimensionless threadline velocity for the three cases shown in (23).

curve in Fig. 1, if the value of $\xi = v/v_o$ at the position of the maximum x/L is less than r (or equivalently, the curve of $\xi = v/v_o$ has an excursion beyond the point of x/L = 1), then there are always multiple (double) values of $\xi = v/v_o$ at x/L = 1 because of the fixed boundary condition at the take-up as shown by Eqn. (10).

Hence at the point of maximum value of x/L, we have

$$d(x/L)/d\xi = 0 = \{[1+\beta(r-1)]/\ln r\}(1/\xi) - \beta$$

or

$$\xi = [1+\beta(r-1)]/(\beta \ln r) \tag{19}$$

Therefore, the necking condition is

$$\{[1+\beta(r-1)]/(\beta \ln r)\} < r \tag{20}$$

We can further rewrite the above condition in a simpler form by defining the critical value of β, β_c, at the onset point of the multiple values of ξ (discontinuity of ξ) at the take-up.

$$\{[1+\beta_c(r-1)]/(\beta_c \ln r)\} = r,$$

or

$$\beta_c = 1/[r(\ln r - 1) + 1] \tag{21}$$

Then the necking condition of Eqn. (20) becomes

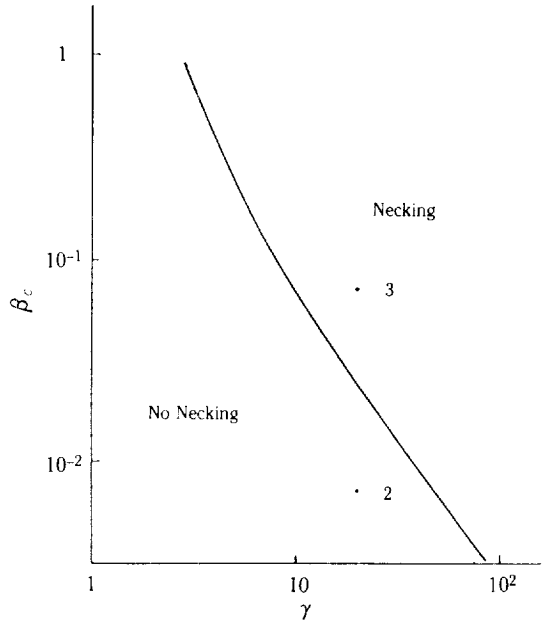

Fig. 2. Necking condition curve and the three cases.

$$\beta > \beta_c(r) = 1/[r(\ln r - 1) + 1] \tag{22}$$

As seen in Fig. 2, β_c is always positive. And so if $\beta < 0$ [i.e., $a < 1/\sqrt{3}$ from Eqn. (13)], the necking condition of Eqn. (22) is never met and thus there is no necking at all. Accordingly, necking is possible only when $\beta > 0$ (i.e., $a > 1/\sqrt{3}$) and Eqn. (22) is satisfied. This means that if the value of β is above the curve of $\beta_c(r)$ as shown in Fig. 2, there occurs necking, whereas if the point of β lies below the curve, no necking results.

In order to demonstrate the situation, we consider three representative cases throughout this study. The same value of r and thus the same $\beta_c(r)$ value are used for the three cases while different values for the material parameter "a" and for the dimensionless relaxation time, $\tilde{\lambda}_o = \lambda_o v_o / L$ are used.

case (1) : $r = 20$, $\beta_c = 0.0244$,
$a = 0.3$ (i.e., $a < 1/\sqrt{3} = 0.577$), $\tilde{\lambda}_o = 0.01$,
$\beta = -0.0048$

case (2) : $r = 20$, $\beta_c = 0.0244$,
$a = 1.0$ (i.e., $a > 1/\sqrt{3}$), $\tilde{\lambda}_o = 0.01$,
$\beta = 0.00732$

case (3) : $r = 20$, $\beta_c = 0.0244$,
$a = 1.0$ (i.e., $a > 1/\sqrt{3}$), $\tilde{\lambda}_o = 0.1$,
$\beta = 0.0732$ (23)

As explained above, case (1) doesn't exhibit necking because β is negative (equivalently $a < 1/\sqrt{3}$) and so the necking condition, Eqn. (22) is not satisfied. Case

(2) also exhibits no necking, because although β is positive ($a>1/\sqrt{3}$), it still is smaller than β_c and so Eqn. (22) is not satisfied. Case (3) does exhibit necking because Eqn. (22) is satisfied. Figs. 1 and 2 show these three cases.

Before moving to the next section of extensional viscosity, we compare the necking condition of melt spinning derived in this section with the conventional necking of solids already mentioned in the Introduction of this article.

There are two conditions for the necking of solids; 1) the material should possess a multi-valued stress-strain curve (i.e., multiple different strain values exist for a single stress) for a certain region of the stress, and 2) the applied stress is greater than the material critical necking stress which depends on both the material characteristics and processing conditions. In parallel with these, for the necking in spinning as derived so far, we can say that $a>1/\sqrt{3}$ or $\beta>0$ corresponds to the first condition above and Eqn. (22) to the second condition. While the first correspondence is easily understood, the second correspondence requires the following illustration.

Combining Eqns. (5), (8), (12), and (13), we get

$$\begin{aligned}\sigma &\equiv F/A \\ &\equiv 2Gv/K = \{(2G\tilde{\lambda}_o \ln r)/[1+\beta(r-1)]\}(v/v_o) \\ &= [(2G\beta \ln r)/\{(a\sqrt{3}-1)[1+\beta(r-1)]\}](v/v_o)\end{aligned} \tag{24}$$

Then the applied stress at the take-up becomes

$$\begin{aligned}\sigma &= [2G\beta(\ln r)r]/\{(a\sqrt{3}-1)[1+\beta(r-1)]\} \\ &= (\text{positive constant})\{1/[(1/\beta)+(r-1)]\}\end{aligned} \tag{25}$$

for given "a", r, and G. The critical necking stress becomes

$$\begin{aligned}\sigma_c &= [2G(\ln r)r\beta_c]/\{(a\sqrt{3}-1)[1+\beta_c(r-1)]\} \\ &= (\text{positive constant})\{1/[(1/\beta_c)+(r-1)]\}\end{aligned} \tag{26}$$

Therefore, the necking condition Eqn. (22) leads to

$$\sigma > \sigma_c \tag{27}$$

i.e., the applied stress>the necking stress, thus proving the second correspondence between necking of solids and necking in spinning.

Finally, we also can find the necking ratio at the take-up as follows.

$$\text{necking ratio} = r/(v/v_o)_{x/L=1} \tag{28}$$

For example, the case (3) which exhibits necking at the take-up, shows that

necking ratio $\simeq 20/5.15 = 3.883$

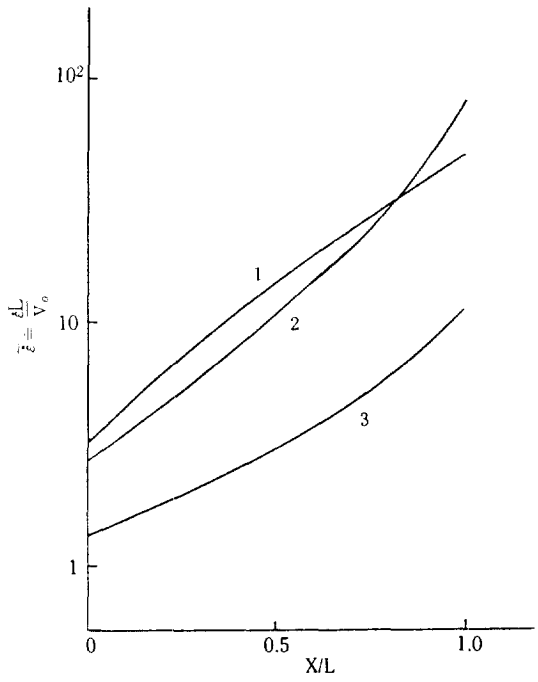

Fig. 3. Eulerian plots of dimensionless extensional strain-rate for the three cases.

DERIVATION OF THE EXTENSIONAL VISCOSITY IN ISOTHERMAL SPINNING

First we need the expression of strain-rate, $\dot{\varepsilon}$, in spinning because the extensional viscosity is defined as the ratio of stress to strain-rate. Combining Eqns. (7) and (12), we get

$$\begin{aligned}\dot{\varepsilon} &\equiv dv/dx \\ &= v/\{\lambda_o[(v_o/v)(1+\beta(r-1))/(\tilde{\lambda}_o \ln r)] + v(1-a\sqrt{3})\} \\ &= 1/[\{L[1+\beta(r-1)]/(v \ln r)\}(1-\lambda_o(a\sqrt{3}-1))]\end{aligned} \tag{29}$$

The dimensionless strain-rate, $\tilde{\varepsilon}$, is then

$$\begin{aligned}\tilde{\varepsilon} &\equiv \dot{\varepsilon}L/v_o \\ &= 1/[\{[1+\beta(r-1)]/\ln r\}(v_o/v) - \tilde{\lambda}_o(a\sqrt{3}-1)] \\ &= 1/[\{[1+\beta(r-1)]/\ln r\}(1/\xi) - \beta]\end{aligned} \tag{30}$$

where $\tilde{\lambda}_o$, β, and ξ are given by Eqns. (13) and (15).

Next, the stress expression is already given by Eqn. (24), and thus the dimensionless stress becomes

$$\begin{aligned}\tilde{\sigma} &\equiv \sigma/(2G) = \tilde{\lambda}_o(\ln r)\xi/[1+\beta(r-1)] \\ &= \beta(\ln r)\xi/\{(a\sqrt{3}-1)[1+\beta(r-1)]\}\end{aligned} \tag{31}$$

Finally the dimensionless extensional viscosity is then obtained from Eqns. (30) and (31).

$$\begin{aligned}\tilde{\eta}_e &\equiv \tilde{\sigma}/\tilde{\varepsilon} = \{\tilde{\lambda}_o(\ln r)\xi/[1+\beta(r-1)]\} \\ &\quad [\{[1+\beta(r-1)]/\ln r\}(1/\xi)-\beta]\end{aligned} \tag{32}$$

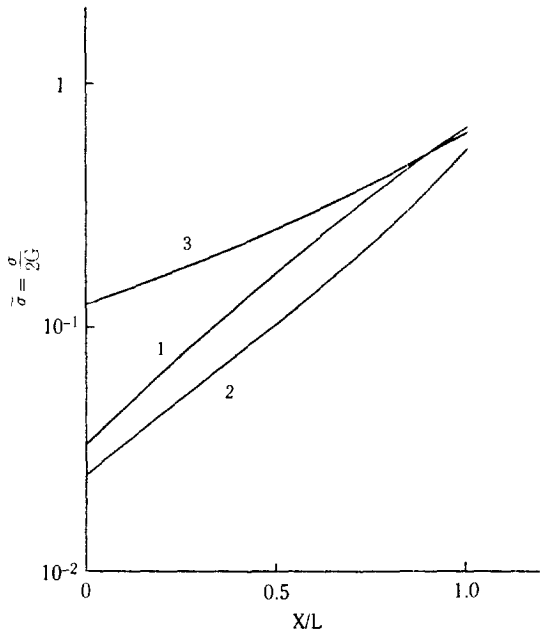

Fig. 4. Eulerian plots of dimensionless threadline stress for the three cases.

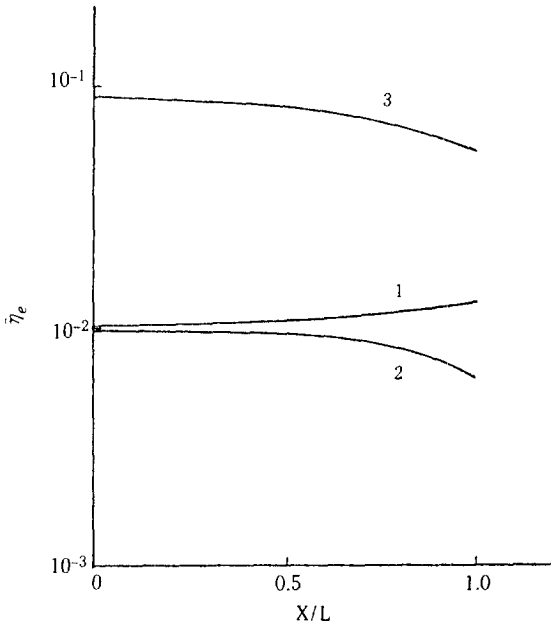

Fig. 5. Eulerian plots of dimensionless extensional viscosity for the three cases.

The above expression is further rewritten as follows. From Eqn. (30) we get

$$\tilde{\xi} = \{1+\beta(r-1)\}/\{\ln r\,[(1/\tilde{\varepsilon})+\beta]\} \tag{33}$$

Substitution of Eqn. (33) into Eqn. (32) yields

$$\tilde{\eta}_e = \tilde{\lambda}_o\{1-\beta/[(1/\tilde{\varepsilon})+\beta]\} = \tilde{\lambda}_o\left\{1-\frac{1}{\frac{1}{\beta\tilde{\varepsilon}}+1}\right\} \tag{34}$$

Now we obtain for given values of $\tilde{\xi}$, the values of the dimensionless strain-rate, $\tilde{\varepsilon}$, dimensionless stress, $\tilde{\sigma}$, and dimensionless extensional viscosity, $\tilde{\eta}_e$, for the same three cases shown in Eqn. (23) using Eqns. (30), (31), and (32) [or (34)], respectively. Then we plot them against the distance from the spinneret using Eqn. (14), i.e., Eulerian plots, and the results are shown in Figs. 3,4, and 5. As we might expect from the velocity profiles in Fig. 1, the strain-rate and stress increase with the distance in isothermal spinning as Figs. 3 and 4 show.

However, the extensional viscosity displays different behavior as shown in Fig. 5, i.e., it increases for case (1) where $a<1/\sqrt{3}$ (or $\beta<0$) whereas it decreases for cases (2) and (3) where $a>1/\sqrt{3}$ (or $\beta>0$). In order to better understand this dichotomy of the cases depending upon the value of "a", this time we plot the same extensional viscosity against the strain-rate and the results are shown in Fig. 6.

The extensional viscosity exhibits strain-thickening (hardening) behavior for the spinning of $a<1\sqrt{3}$ fluids,

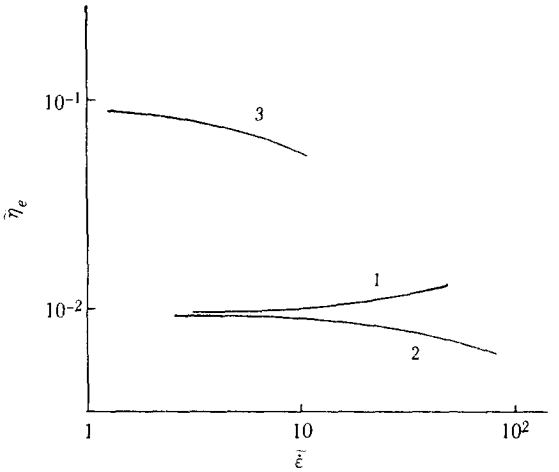

Fig. 6. Dimensionless extensional viscosity vs. dimensionless extensional strain-rate or the three cases.

and strain-thinning (softening) behavior for the spinning of $a>1/\sqrt{3}$ fluids. This is a very important finding, the significance of which will be further discussed in the next section in connection with other flow situations.

We can easily ascertain the above strain-rate dependency of the extensional viscosity from Eqn. (34) as follows. The slope of the curves in Fig. 6 is obtained below.

$$(\partial\bar{\eta}_e/\partial\dot{\varepsilon}) = (-\bar{\lambda}_o(-1/\beta)(-1/(\dot{\varepsilon})^2)/[(1/\beta\dot{\varepsilon})+1]^2$$
$$= -(\bar{\lambda}_o(1/\dot{\varepsilon})^2/[(1/\beta\dot{\varepsilon})+1]^2)(1/\beta)$$
$$= -(\text{positive constant})(1/\beta) \quad (35)$$

Thus the slope becomes positive (strain-hardening), if $\beta<0$ [as in case (1) curve], and negative (strain-softening), if $\beta>0$ [as in cases (2) and (3) curves].

DISCUSSION

In the previous sections, we have derived the necking condition for isothermal spinning, which directly corresponds to the necking condition of solids. We also have found that the extensional viscosity becomes strain-thickening (hardening) or strain-thinning (softening) depending upon the value of "a" (the material parameter representing the degree of the strain-rate dependency of the material relaxation time). Here we further point out that the dichotomy of fluids determined by "a" governs other extensional flow situations as well.

First, we show that $\lambda_o\dot{\varepsilon}$ = dimensionless strain-rate (different from the other dimensionless strain-rate, $\bar{\dot{\varepsilon}}$) = a Deborah number has a maximum value for $a<1/\sqrt{3}$ fluids and no maximum for $a>1/\sqrt{3}$ fluids. From Eqns. (7) and (29), we find that

$$\lambda_o K\dot{\varepsilon}+\lambda_o v(1-a\sqrt{3})\dot{\varepsilon}=v, \text{ or}$$
$$v=(\lambda_o K\dot{\varepsilon})/[1+\lambda_o(a\sqrt{3}-1)\dot{\varepsilon}] \quad (36)$$

Since the numerator is always positive in spinning, the denominator should be positive to make v positive. Hence, the fluids having $a>1/\sqrt{3}$ set no condition on $\lambda_o\dot{\varepsilon}$, whereas the fluids having $a<1/\sqrt{3}$ yield the maximum value of $\lambda_o\dot{\varepsilon}$ as follows.

$$(\lambda_o\dot{\varepsilon})_{max}=1/(1-a\sqrt{3}) \quad (37)$$

Thus we have found that in the constant force extension (i.e., spinning processes), there exists the maximum extension rate for strain-hardening fluids while no maximum extension rate exists for strain-softening fluids. Denn and Marrucci [11] derived the similar results for constant strain-rate extension. Ide and White [10] interpreted these as cohesive failure mode and ductile failure mode (necking), respectively.

Following the similar approach, we can find the maximum extension (i.e., the maximum draw-down ratio, r) for strain-hardening fluids and no such maximum value of r for strain-softening fluids as shown below. From Eqn. (12), we have

$$K=v_o(1+\beta)(r-1)/(\bar{\lambda}_o\ln r)=v_o(1+\bar{\lambda}_o(a\sqrt{3}-1)(r-1)]/(\bar{\lambda}_o\ln r)$$

While the strain-softening ($a>1/\sqrt{3}$) fluids always make K positive and so no condition on r, the strain-hardening ($a<1/\sqrt{3}$) fluids make K positive only when r is smaller than r_{max} given by

$$r_{max}=1+1/[\bar{\lambda}_o(1-a\sqrt{3})] \quad (38)$$

The case of a = 0 (constant relaxation time) was reported by Hyun & Ballman [8] for the result of Eqn. (37) and Hyun [7] for the result of Eqn. (38).

Secondly, the finding in this study that the extensional viscosity can become either strain-hardening or strain-softening has already been observed experimentally by Chen et al. [12], Kanai & White [13], Tsou & Bogue [14] and others using LDPE, HDPE, etc. in spinning and tubular film blowing experiments. Our theoretically derived results of the phenomenon and the necking conditions here corroborate their data fairly well. The theoretical results by Ide & White [10] and Minoshima & White [15] about the different failure modes of the various polymer melts [i.e., necking (ductile failure mode) and no necking (cohesive failure mode)] also render good agreement with our results.

Thirdly, the respective correspondence between the necking (or no necking) in spinning and no vortex (or vortex) in entrance flow deserves some discussion. Recently, Baird et al. [16] and Binding [17] and others have found that the vortex formation in entrance flow (contraction flow) is related to the strain-hardening behavior of the extensional viscosity.

As shown in Fig. 8, it is intuively clear that if the fluid can perform necking in extensional flow, there is

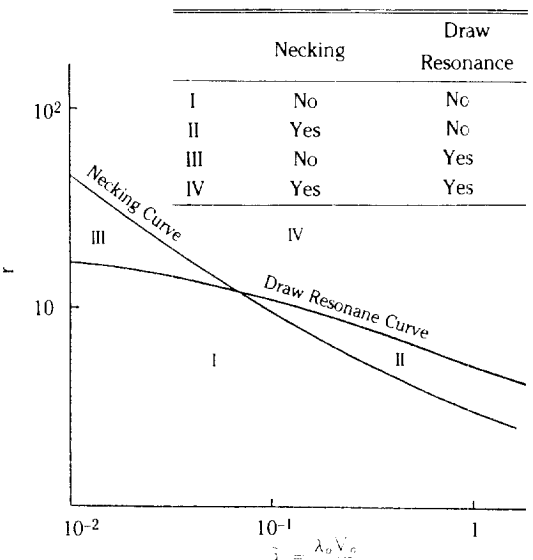

Fig. 7. Necking curve and draw resonance curve in spinning of a strain-softening fluid: case (3).

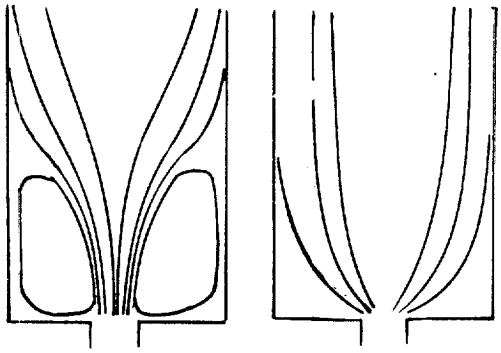

Fig. 8. Schematic diagram of entrance flow, (a) vortex formed (b) no vortex.

no vortex in entrance flow [Fig. 8(b)], while if the fluid exhibits no necking in extensional flow, then vortex is inevitable [Fig. 8(a)], because smooth extensional flow profiles (so-called wine glass-shaped profiles) are formed as a stress relieving mechanism. Hence, we can say that necking in spinning and vortex in entrance flow are governed by basically the same extensional flow mechanism which is determined by the extension rate dependency of the extensional viscosity, which, in turn, is decided by the dichotomy of the fluids according to the material parameter "a" in this study.

Fourthly, as reported by Hyun [9], the draw resonance phenomenon in spinning also displays fundamentally different behavior depending upon the value of "a". Since strain-softening ($a>1/\sqrt{3}$) fluids can exhibit necking if the necking condition of Eqn. (22) is satisfied, we plot the necking curve and draw resonance curve in the same figure for the case (3) in Fig. 7. There are four different regions as to whether necking and draw resonance can occur. While some experimental data exist for some regions, there are not yet complete experimental results to explain fully the whole region of Fig. 7.

CONCLUSION

The crux of the results of this study is that the dichotomy of fluids reveals 1) necking in spinning, 2) vortex in entrance flow, 3) draw resonance in spinning, and 4) failure modes of extension of solids, are all

Table 1. Comparison of the two fluids

Categories	Fluids I	Fluids II
Strain-rate dependence of the material relaxation time, "a"	small, $a<1/\sqrt{3}$	large, $a>1/\sqrt{3}$
Necking in spinning	necking impossible	necking possible if necking condition of Eqn. (22) satisfied
Draw resonance in spinning	r_c is larger than 20.21 (Newtonian r_c) and increases with $\tilde{\lambda}_o$	r_c is smaller than 20. 21 (Newtonian r_c) and decreases with λ_o
Strain-rate dependence of the extensional viscosity	strain-thickening (hardening)	strain-thinning (softening)
Vortex in entrance flow	vortex formed	no vortex
Failure mode of solid extension	cohesive failure mode	ductile failure mode (necking)
Effect of $\tilde{\lambda}_o \equiv \frac{\lambda_o V_o}{L}$ on necking	no effect (no necking)	more necking
Effect of $\tilde{\lambda}_o \equiv \frac{\lambda_o V_o}{L}$ on draw resonance	stabilizing (or reduce draw resonance)	destabilizing (or increase draw resonance)
Effect of r = draw-down ratio on necking	no effect (no necking)	more necking
Effect of r on draw resonance	increase draw resonance	increase draw resonance
Multiplicity in capillary flow rate	no multiplicity	multiplicity
Typical materials	LDPE	HDPE
Maximum dimensionless extension rate, $(\lambda_o \dot{\varepsilon})_{max}$	$1/(1-a\sqrt{3})$	Doesn't exist
Maximum draw-down ratio, r_{max}	$1+1/[\tilde{\lambda}_o(1-a\sqrt{3})]$	Doesn't exist

related to each other and are governed by the behavior of the same extensional viscosity in extensional flow. Therefore, the conclusion can be best summarized by Table 1 below where the comparison of two different fluids in different flow situations, is made. What we have shown in this article is thus that using a simple model which is amenable to analytical calculation, the fundamental physics involved in extensional flow, is revealed and interpreted. There are, of course, many tasks left in studying extensional flow, e.g., instead of a single material relaxation time, multiple relaxation times, and more accurate constitutive equation, etc., which obviously require extensive computer simulation efforts.

NOMENCLATURE

- A : threadline cross-sectional area
- a : material parameter representing the strain-rate dependence of the material relaxation time
- F : threadline tension force
- G : material modulus
- K : threadline reciprocal force, $K \equiv 2\,G\,Q/F$
- L : distance from spinneret to take-up
- Q : threadline throughput (flow rate), $Q = Av$
- r : draw-down ratio, $r = v_L/v_o = A_o/A_L$
- r_c : critical r at the onset of draw resonance
- t : time
- v : threadline velocity
- v_o : threadline velocity at spinneret ($x = 0$)
- v_L : threadline velocity at take-up ($x = L$)
- x : distance from spinneret
- β : dimensionless term, $\beta \equiv \tilde{\lambda}_o\,(a\sqrt{3} - 1)$
- β_c : value of β at critical necking situation
- $\dot{\varepsilon}$: extensional strain-rate
- $\tilde{\dot{\varepsilon}}$: dimensionless extensional strain-rate, $\tilde{\dot{\varepsilon}} \equiv \dot{\varepsilon} L/v_o$
- η_e : extensional viscosity, $\eta_e \equiv \sigma/\dot{\varepsilon}$
- $\tilde{\eta}_e$: dimensionless extensional viscosity, $\tilde{\eta}_e \equiv \tilde{\sigma}/\tilde{\dot{\varepsilon}}$
- λ : material relaxation time
- λ_o : constant materials relaxation time
- $\tilde{\lambda}_o$: dimensionless material relaxation time, $\tilde{\lambda}_o \equiv \lambda_o\, v_o/L$
- ξ : dimensionless threadline velocity, $\xi \equiv v/v_o$
- σ : threadline stress
- σ_c : critical necking stress
- $\tilde{\sigma}$: dimensionless threadline stress, $\tilde{\sigma} = \sigma / (2G)$
- τ : fluid traveling time from spinneret
- $\tilde{\tau}$: dimensionless fluid traveling time from spinneret, $\tilde{\tau} = \tau\, v_o/L$

REFERENCES

1. Vincent, P.I.: *Polymer*, **1,** 7 (1960).
2. Wada, Y.: *J. Appl. Poly. Sci.*, **15,** 183 (1971).
3. Ziabicki, A.: "Fundamentals of Fibre Formation", John Wiley & Sons, New York, p. 69 (1976).
4. Kase, S.: Proceedings of Poly. Processing Soc., No. 3/17, Orlando, (1988).
5. Maeda, Y.: Proceedings of Poly. Processing Soc., No. 3/18, Orlando, (1988).
6. Kikutani, I., et al.: Proceedings of Poly. Processing Soc., No. 3/19, Orlando, (1988).
7. Hyun, J.C.: *AIChE J.*, **24,** 418 (1978).
8. Hyun, J.C. and Ballman, R.L.: *J. Rheology*, **22,** 349 (1978).
9. Hyun, J.C.: *Polymer* (Korea), **12,** 772, (1988).
10. Ide, Y. and White, J.L.: *J. Non-Newtonian Fluid Mech.*, **2,** 281 (1977).
11. Denn, M.M. and Marrucci, G.: *AIChE J.*, **17,** 101 (1971).
12. Chen, I.-J., et al.: *Transactions of Soc. of Rheology*, **16,** 473 (1972).
13. Kanai, T. and White, J.L.: *Poly. Eng. & Sci.*, **24,** 1185 (1984).
14. Tsou, J.-D. and Bogue, D.C.: *J. Non-Newtonian Fluid Mech.*, **17,** 331, (1985).
15. Minoshima, W. and White, J.L.: *J. Non-Newtonian Fluid Mech.*, **19,** 275 (1986).
16. White, S.A., Gotsis, A.D., and Baird, D.G.: *J. Non-Newtonian Fluid Mech.*, **24,** 121, (1987).
17. Binding, D.M.: *J. Non-Newtonian Fluid Mech.*, **27,** 173 (1988).